

# Modern control of linear global instability in a cylinder wake model

Eric Lauga <sup>\*,1</sup>, Thomas R. Bewley

*Department of Mechanical and Aerospace Engineering, University of California San Diego, La Jolla, CA 92093, USA*

## Abstract

This article investigates the implementation of modern control design techniques on models of open shear flows using the linear complex Ginzburg–Landau (GL) model for the cylinder wake, with the coefficients as scaled by Roussopoulos and Monkewitz (Physica D 97 (1996) 264). Based on noisy measurements 1.5 diameters downstream of the cylinder, the compensator uses an  $\mathcal{H}_\infty$  filter to construct a state estimate which, in turn, is used to compute  $\mathcal{H}_\infty$  feedback control at the cylinder to drive the system perturbations to zero. The application of such modern control rules leads to substantially better performance than the proportional measurement feedback proposed by previous studies. Preliminary results of the effectiveness of linear control to stabilize the nonlinear GL model are also presented. © 2002 Elsevier Science Inc. All rights reserved.

PACS: 47.20.-k; 47.20.Ft; 47.62.+q

Keywords: Hydrodynamic stability; Instability of shear flows; Flow control

## 1. Introduction

The instability and self-sustained oscillation of the flow behind a circular cylinder is a fundamental yet only recently understood problem. Due to the numerous engineering consequences of unstable bluff-body flows, the canonical problem of the instability of the cylinder wake has been the focal point of many studies in the past decade (see, e.g., Williamson, 1996 for a review). The possibility of controlling this instability, or at least delaying the critical value of Reynolds number characterizing its onset, is an idea that has recently received growing attention (see, e.g., Tokumaru and Dimotakis, 1991; Min and Choi, 1999; He et al., 2000).

Experimental and numerical studies of control of vortex shedding have been the focus of several investigations. As early as 1967, proportional measurement feedback control of vortex shedding behind an oblong cylinder was implemented experimentally in Berger (1967); he succeeded for a short range of Reynolds numbers, between  $Re_c = 79.2$  and  $Re = 90.3$ . Since then,

many other publications have considered various passive and physically-based active strategies. A numerical and theoretical study of the control of the cylinder wake has been carried out in Park et al. (1994). Using proportional measurement feedback, suppression of vortex shedding was achieved in their simulations at  $Re = 60$  for select sensor locations. At  $Re = 80$ , the wake could not be controlled; the primary vortex shedding mode was stabilized but a secondary, lower-frequency shedding mode arose; this effect was also observed experimentally by Roussopoulos (1993). More recently, Min and Choi (1999) used “suboptimal” control theory (i.e. finite-horizon nonlinear optimal control theory applied over an infinitesimal time horizon, subject to several convenient assumptions) to completely stabilize vortex shedding in simulations up to  $Re = 160$ . This impressive performance well exceeds previous results and motivates the present work, which attempts to stabilize a model of the wake using simpler, time-independent feedback gains.

The growing flow control community and the interdisciplinary perspective it has pursued in the last few years makes it now possible to adapt a modern control point of view on certain flow systems. We have recently published an extensive review article (Bewley, 2001) that provides a basic introduction to certain well-known concepts from modern control theory in the fluid-mechanical setting, defining transfer function norms,

\* Corresponding author. Present address: Division of Engineering and Applied Sciences, Harvard University.

E-mail address: lauga@deas.harvard.edu (E. Lauga).

<sup>1</sup> This work was done in collaboration with LadHyX, Laboratoire d’Hydrodynamique, Ecole Polytechnique, France.

### Nomenclature

|                      |                                      |                              |   |
|----------------------|--------------------------------------|------------------------------|---|
| $\mathcal{H}_2$      | optimal control                      | $\mathbf{w}$                 | disturbance vector                                |
| $\mathcal{H}_\infty$ | robust control                       | $A$                          | GL operator discretization matrix                 |
| $Re$                 | Reynolds number                      | $B_1$                        | state disturbances input matrix                   |
| $\psi$               | state variable                       | $D_{12}$                     | measurement noise input matrix                    |
| $t$                  | time coordinate                      | $B_2$                        | control input matrix                              |
| $x$                  | space coordinate                     | $C_1$                        | measurement output matrix                         |
| $\mu$                | instability term in the GL equation  | $\alpha$                     | noise to disturbance ratio                        |
| $U$                  | coefficient of advection term        | $\ell$                       | control penalty                                   |
| $\eta$               | coefficient of diffusion term        | $\gamma$                     | robustness parameter                              |
| $\lambda$            | coefficient of nonlinear term        | $\mathcal{J}$                | cost functional                                   |
| $w_\psi$             | state disturbances                   | $Q$                          | state energy matrix                               |
| $w_y$                | measurement noise                    | $R$                          | control energy matrix                             |
| $y$                  | measurement output                   | $S$                          | disturbance energy matrix                         |
| $u$                  | control input                        | $\ T_{\mathbf{xw}}\ _2$      | transfer function 2-norm                          |
| $x_f$                | actuator position                    | $\ T_{\mathbf{xw}}\ _\infty$ | transfer function $\infty$ -norm                  |
| $x_s$                | sensor position                      | $\Delta_2$                   | relative gain in $\ T_{\mathbf{xw}}\ _2$ (%)      |
| $\mathbf{x}$         | state variable discretization vector | $\Delta_\infty$              | relative gain in $\ T_{\mathbf{xw}}\ _\infty$ (%) |

state feedback, estimators, etc., and providing an introduction to  $\mathcal{H}_\infty$  control theory and the separation principle of the  $\mathcal{H}_2$  setting. This review article provides scores of references to related work at the intersection of these two fields. The present paper assumes knowledge of this review article as background material, and investigates the use of linear  $\mathcal{H}_\infty$  control theory on a 1D model of the cylinder wake in order to shed some light on some of the central unsolved issues in the control of instabilities in open shear flows.

Open shear-flow instabilities, and the major role they play in flow transition, have been analyzed in the last 15 years using the concepts of absolute and convective instabilities (Huerre and Monkewitz, 1990). Considering an unstable parallel flow, the instability is called convective if a perturbation grows while being advected away by the mean flow and any fixed point in the domain eventually comes back to rest when the upstream disturbance is removed. On the other hand, if the mean advection is not strong enough, the instability will contaminate the entire system and is called absolute; in this case, the flow perturbation remains even if the disturbance triggering it is neutralized. These characterizations of parallel flows can be extended to the local analysis of slightly nonparallel flows. Nonparallel flows are often found to contain different regions with different stability characteristics. Flows which are locally convectively unstable everywhere behave as noise amplifiers, as they are extremely sensitive to external disturbances, though they are globally stable. On the other hand, flows displaying a sufficiently large pocket of absolute instability behave as oscillators (Chomaz et al., 1988), and are found to be dominated by a synchronized linear behavior, termed a linear global mode. This linear

transient will grow in place and eventually saturate due to nonlinearities, leading to self-sustained oscillations such as those in the wake of the circular cylinder.

## 2. The Ginzburg–Landau model

The system we will consider in this paper, the non-parallel Ginzburg–Landau (GL) system, is the simplest model one can construct that displays a spatial transition from a local convective instability to a local absolute instability. It is given by

$$\frac{\partial \psi}{\partial t} = \left( \mu(x) - U(x) \frac{\partial}{\partial x} + \eta \frac{\partial^2}{\partial x^2} \right) \psi - \lambda |\psi|^2 \psi. \quad (1)$$

This equation models the wave amplitude in a spatially extended system and has been used successfully to model the transition of both closed and open flows. In the case of interest here, the coefficients  $\mu(x)$ ,  $U(x)$  and  $\eta$ , and their dependence on the Reynolds number, are chosen such that this equation models quantitatively the Hopf bifurcation which takes place in the cylinder wake at  $Re = 47$  and qualitatively the wake behavior as the Reynolds number is increased beyond this value. The present paper focuses primarily on the control and estimation of the linear GL equation (linearizing the system around the solution  $\psi = 0$ ); we will also characterize the effect of this linear control on the global nonlinear behavior. We choose complex coefficients in (1) and the dependence of these coefficients on Reynolds number as suggested by Roussopoulos and Monkewitz (1996) in their study of the cylinder wake feedback control problem to facilitate comparison with the existing literature.

### 3. The control strategy

This work addresses the following idealized model problem displayed in Fig. 1: considering the 1D system model (1), what stabilizing effect can be achieved with noisy information about the system 1.5 diameters downstream of the origin and actuation at the origin (i.e., the cylinder location) itself, even if the system is perturbed by unknown external disturbances and significant unmodeled system dynamics? The actuation might be achieved in practice by rotation or transverse oscillation of the cylinder itself; we do not attempt to model accurately the flow actuation in our present 1D analysis, which is focused more on the alteration of the global dynamics in the 1D model of the wake. We represent the control  $u$  as a local forcing at  $x = x_f$  and the measurement  $y$  of the state of the system at  $x = x_s$  such that we may represent the linearization of the model (1) as:

$$\frac{\partial \psi}{\partial t} = \mathcal{L}\psi + w_\psi(x, t) + \delta(x - x_f)f(t),$$

$$y = \psi(x_s) + w_y(t),$$
(2)

where  $\mathcal{L}$  functionally represents the first three terms on the right-hand side of (1), and  $w_\psi(x, t)$  and  $w_y(t)$  represent the state disturbances and measurement noise respectively. As in Roussopoulos and Monkewitz (1996), we take  $x_f = 0$  and  $x_s = 1.5$ . Fig. 2 displays the position of both the actuator and the sensor with respect to the local instability zones of the uncontrolled system for a variety of Reynolds numbers. An appropriate discretization of the continuous GL equation leads to the standard state-space form for the system. Taking  $\alpha$  as a free parameter representing the ratio of the strength of the measurement noise to that of the state disturbances, we write this state-space form as

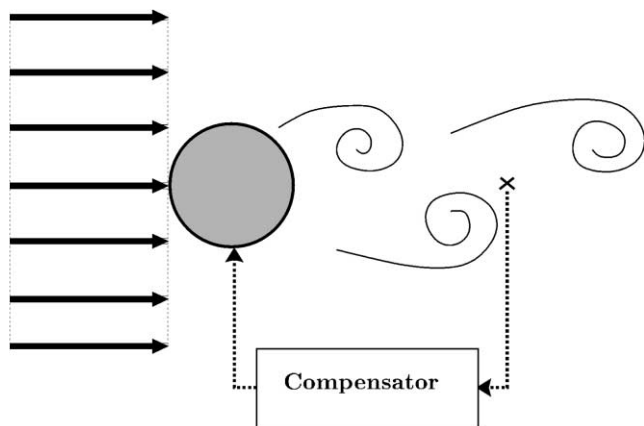


Fig. 1. Vortex shedding control approximately modeled by the idealized 1D system: based on noisy measurements downstream of the cylinder, the compensator constructs a state estimate which, in turn, is used to compute control feedback applied at the cylinder itself.

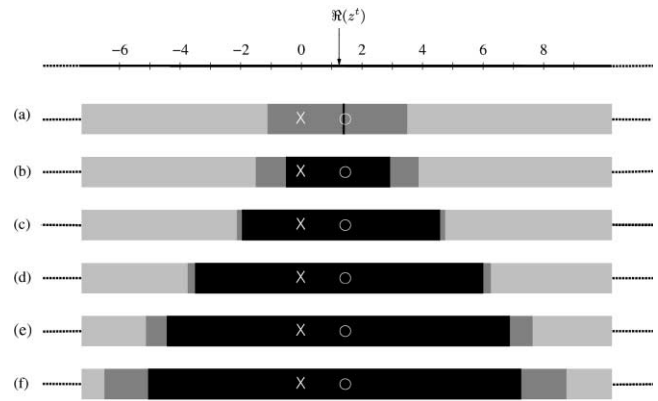


Fig. 2. Sketches on the region on the real  $x$ -axis of local stability (light grey), convective instability (dark grey) and absolute instability (black) of the uncontrolled GL model for various Reynolds numbers. (a)  $Re = 29$ , onset of local absolute instability at  $x = 1.24$  (b)  $Re = 47$ , onset of linear global instability, (c)  $Re = 100$ , (d)  $Re = 175$ , (e)  $Re = 235$ , (f)  $Re = 284$ . Representative locations for the sensor and actuator are marked with  $o$  and  $\times$  respectively; we seek to determine control forcing, to be applied at  $x_f$ , based on the sensor measurement, taken at  $x_s$ , in order to stabilize the global dynamics of this system.

$$\dot{\mathbf{x}} = A\mathbf{x} + B_1\mathbf{w} + B_2u,$$

$$y = C_1\mathbf{x} + \alpha D_2\mathbf{w},$$
(3)

where  $\mathbf{x}$  is the discretized state vector,  $u$  the control, and  $\mathbf{w}$  the discretized disturbance vector (including both the measurement noise and the state disturbances). The computations presented in this paper have been achieved with a Fourier collocation method for the spatial discretization on a stretched grid clustered near both the sensor and forcing points to ensure resolution of the sensing and forcing. The control design applied by our study is the linear  $\mathcal{H}_\infty$  control approach introduced by Doyle et al. (1989). This control methodology can be briefly described as the following: (1) choice of a quadratic cost function, (2) choice of the design parameters, and (3) computation of the control matrices. The performance of the closed-loop plant depends strongly on the several decisions made at each of these steps. The cost function  $\mathcal{J}$  must weigh together the state  $\mathbf{x}$ , the control  $u$ , and the noise  $\mathbf{w}$ ; moreover, since the GL operator is time invariant, one can apply the control theory for infinite time horizons, which leads to the following general form for the cost function:

$$\mathcal{J} = \mathcal{E}[\mathbf{x}^* Q \mathbf{x} + \ell^2 u^* R u - \gamma^2 \mathbf{w}^* S \mathbf{w}],$$
(4)

where  $Q$ ,  $R$  and  $S$  are positive definite matrices and  $\mathcal{E}$  denotes the expected value. The  $\mathcal{H}_\infty$  control approach allows one to compute the control  $u$  that minimizes the cost function in the presence of the “worst-case” disturbance  $\mathbf{w}$  that simultaneously maximizes the cost function, in the spirit of a noncooperative game or saddle-point problem. More detailed review of the  $\mathcal{H}_\infty$  control design procedure is given in Bewley (2001). In

addition to  $\alpha$ , the two other design parameters are the weighting on the control penalty,  $\ell$  (large  $\ell$  resulting in small control amplitude), and the weighting on the disturbance penalty,  $\gamma$  (large  $\gamma$  resulting in small “worst-case” disturbance amplitude accounted for during the controller design). A case of particular interest is the  $\mathcal{H}_2$  (or “optimal control”) approach, which is achieved by taking the  $\gamma \rightarrow \infty$  limit, resulting in a worst-case disturbance of vanishing amplitude to be accounted for during the controller design. It may be shown that the control design procedure in this limit is essentially equivalent to the control design that minimizes the cost function under a white-noise assumption for  $\mathbf{w}$ .

#### 4. Performance analysis

In the previous section, we briefly discussed the reformulation of the GL system into standard state-space form and the design an  $\mathcal{H}_\infty$  compensator for this system with three design parameters  $\ell$ ,  $\alpha$ , and  $\gamma$ . This section now examines some of the relevant questions concerning the effectiveness of this compensation on both the linear and the nonlinear GL system.

##### 4.1. Linear control of the linear GL equation

We now introduce three appropriate measures of performance for the present problem. The first measure is the maximum Reynolds number for stability of the closed-loop system using double-precision arithmetic (see Lauga and Bewley, 2002 for further discussion regarding the influence of numerical precision on this result). If one does not apply control, the system is unstable as soon as  $Re$  exceeds the threshold value of 47. The higher the new threshold for instability is, the more effective the control is for delaying transition. The other two performance measures are the transfer function 2-norm  $\|T_{\mathbf{xw}}\|_2$ , quantifying the amplification of zero-mean white Gaussian disturbances by the closed-loop system, and the transfer function infinity-norm  $\|T_{\mathbf{xw}}\|_\infty$ , quantifying the amplification of disturbances with “worst-case” structure by the closed-loop system. Broadly speaking, the transfer-function norms  $\|T_{\mathbf{xw}}\|_2$  and  $\|T_{\mathbf{xw}}\|_\infty$  represent how the wake model with control feedback applied responds to benign and malevolent disturbance respectively. As a consequence,  $\|T_{\mathbf{xw}}\|_2$  for a given stable system is always smaller than  $\|T_{\mathbf{xw}}\|_\infty$ .

Optimal control with full information and double-precision arithmetic stabilizes the wake model up to a Reynolds number  $Re_s = 284$ , which corresponds to stabilization of seven linear global modes. This represents an effective stabilizability limit of the model system with the chosen actuator using double-precision arithmetic. The estimator itself is able to fully recover the state from noisy measurements at  $x_s = 1.5$  up to a Reynolds num-

ber of  $Re_d = 235$ ; this represents an effective detectability limit of the model using the chosen sensor double-precision arithmetic. Due to the separation principle between the control and estimation problems in the  $\mathcal{H}_2$  framework, the compensator formed by combining the estimator and the controller will stabilize the plant up the minimum of these two values,  $Re_c = 235$ . This critical Reynolds number, corresponding to the stabilization of six linear global modes, compares quite favorably with the maximum Reynolds number  $Re = 64$  which could be stabilized by the proportional control approach developed by Roussopoulos and Monkewitz (1996), which stabilized only one linear global mode. Our first conclusion is therefore that the optimal control design is much more effective in delaying system instability than simpler control strategies.

A “robust” control design can also be developed with this approach, either for the full-information case or for the measurement-based compensator. Fig. 3 displays the variations of the effective stabilizability limit using full-information  $\mathcal{H}_\infty$  control and double-precision arithmetic for various values of the control penalty  $\ell$ . Table 1 extends these results to the  $\mathcal{H}_\infty$  compensator, i.e. to the case in which the controller does not have access to full information but instead constructs a state estimate based on the measurement obtained by the sensor.

The results from Fig. 3 and Table 1 allow us to make several important observations. It appears first that the maximum stabilized Reynolds number using double-precision arithmetic depends monotonically on the ro-

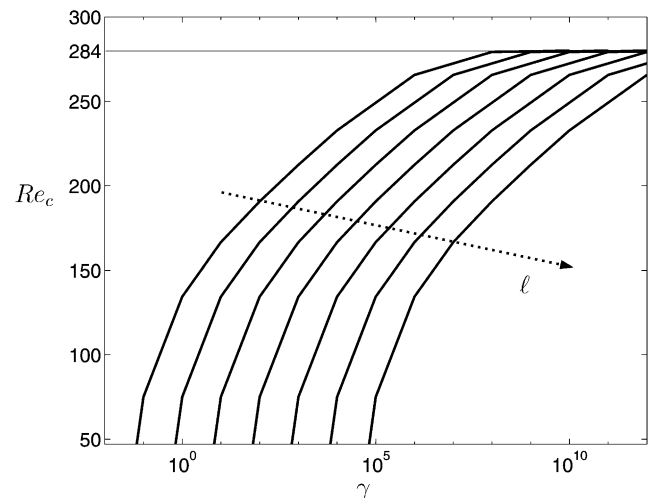


Fig. 3. Maximum Reynolds number for stability of the controlled GL system with full-information  $\mathcal{H}_\infty$  control and double-precision arithmetic as a function of the robustness parameter  $\gamma$  for various values of the control penalty  $\ell$ . The horizontal line represents the  $\mathcal{H}_2$  limit  $Re = 284$  (independent of  $\ell$ ). This plot shows that, for a given value of design-point linear worst-case disturbance rejection  $\gamma$ , an increased value of  $Re_c$  is attained for reduced values of  $\ell$ , at the cost of increased control input.

Table 1

New stability Reynolds  $Re_c$  number for measurement-based  $\mathcal{H}_\infty$  control of the linear GL equation using double-precision arithmetic as a function of the robustness parameter  $\gamma$  for three cases<sup>a</sup>

| log $\gamma$ | $Re_c$ |        |        |
|--------------|--------|--------|--------|
|              | Case 1 | Case 2 | Case 3 |
| 1            | 47.0   | 47.0   | 47.0   |
| 2            | 50.9   | 47.0   | 47.0   |
| 3            | 99.4   | 47.0   | 47.0   |
| 4            | 129.6  | 89.1   | 94.2   |
| 5            | 151.2  | 122.5  | 120.0  |
| 6            | 169.7  | 142.7  | 140.7  |
| 7            | 186.5  | 163.7  | 160.6  |
| 8            | 218.4  | 201.3  | 197.5  |
| 9            | 231.5  | 218.4  | 215.5  |
| 10           | 235.0  | 221.6  | 231.6  |
| $\infty$     | 235.0  | 235.0  | 235.0  |

<sup>a</sup> Case 1:  $\ell = 1, \alpha = 1$ ; Case 2:  $\ell = 1, \alpha = 100$ ; Case 3:  $\ell = 100, \alpha = 1$ ; note that as the design-point linear worst-case disturbance rejection is improved ( $\gamma$  reduced), the new stability Reynolds number deteriorates (reduces).

bustness parameter  $\gamma$  before reaching an asymptotic value. These asymptotic values as  $\gamma$  approaches infinity are the values given by the optimal control approach ( $Re = 284$  for the full-information case in Fig. 3,  $Re = 235$  for the estimator-based case in Table 1), which was expected as the  $\mathcal{H}_2$  control design reduces exactly to the  $\mathcal{H}_\infty$  control design for  $\gamma \rightarrow \infty$ . Another observation is that, for a given robustness parameter  $\gamma$ , increasing the penalty on the control  $\ell$  or the measurement noise strength  $\alpha$  results in decreasing the maximum  $Re$  which is stabilized (a detailed analysis actually shows that the limit on the Reynolds number depends only on the ratio  $\ell/\gamma$  in the case of full-information control, as can be seen on Fig. 3). We see therefore that the  $\mathcal{H}_\infty$  approach is less efficient than the  $\mathcal{H}_2$  control in delaying the instability; introduction of the disturbance effectively detunes the optimal compensator.

Another advantage of the modern control design over the simpler proportional scheme of Roussopoulos and Monkewitz (1996) is the decrease in the transfer function norms. Table 2 presents a comparison at  $Re = 60$  for two different noise strengths between the values of the transfer function 2-norms and infinity-norms for the RM96 proportional approach and for the present optimal control approach with various values for  $\ell$ .

A first result to be observed is the monotonic dependence of the transfer function norms on the control penalty  $\ell$  and the measurement noise to state disturbance ratio  $\alpha$ : for a given  $\alpha$ , increasing  $\ell$  results in less authority of the control and therefore deteriorates the disturbance rejection (increasing the values for the transfer function norms); for a given  $\ell$ , increasing  $\alpha$  results in having less reliable measurements and therefore again deteriorates the disturbance rejection. By analysing the results of Table 2, it is clear that, both in the

Table 2

Comparison of transfer function norms  $\|T_{xw}\|_2$  and  $\|T_{xw}\|_\infty$  at  $Re = 60$  for six types of control<sup>a</sup>

| $\alpha$ | Control                             | $\ T_{xw}\ _2$ | $\ T_{xw}\ _\infty$ |
|----------|-------------------------------------|----------------|---------------------|
| 0.01     | RM96 (proportional)                 | 55.8           | 653                 |
|          | $\mathcal{H}_2$ ( $\ell = 10,000$ ) | 21.0           | 130                 |
|          | $\mathcal{H}_2$ ( $\ell = 100$ )    | 20.3           | 122                 |
|          | $\mathcal{H}_2$ ( $\ell = 10$ )     | 12.1           | 44.1                |
|          | $\mathcal{H}_2$ ( $\ell = 1$ )      | 8.0            | 18.0                |
|          | $\mathcal{H}_2$ ( $\ell = 0.01$ )   | 7.6            | 15.0                |
| 100      | RM96 (proportional)                 | 212            | 2500                |
|          | $\mathcal{H}_2$ ( $\ell = 10,000$ ) | 165            | 1343                |
|          | $\mathcal{H}_2$ ( $\ell = 100$ )    | 161            | 1308                |
|          | $\mathcal{H}_2$ ( $\ell = 10$ )     | 121            | 796                 |
|          | $\mathcal{H}_2$ ( $\ell = 1$ )      | 99.4           | 582                 |
|          | $\mathcal{H}_2$ ( $\ell = 0.01$ )   | 96.8           | 553                 |

<sup>a</sup> The proportional strategy of Roussopoulos and Monkewitz (1996), measurement-based  $\mathcal{H}_2$  control for  $\ell = 10,000, 100, 10, 1$  and  $0.01$ . Top:  $\alpha = 0.01$ , bottom:  $\alpha = 100$ ; note that  $\mathcal{H}_2$  control uniformly improves both measures of disturbance rejection as compared with proportional control.

case of low ( $\alpha = 0.01$ ) and high ( $\alpha = 100$ ) noise strength, applying modern control on the present system is more effective than proportional control in terms of disturbance rejection in the closed-loop system, both for rejection of “white” disturbances (reduced values of  $\|T_{xw}\|_2$ ) and for rejection of “worst-case” disturbances (reduced values of  $\|T_{xw}\|_\infty$ ). Therefore, even in the domain where the simple proportional control of RM96 stabilizes the model, it is much preferable to apply modern control.

A final important aspect to be considered in this linear study is the relative performance of the  $\mathcal{H}_2$  and  $\mathcal{H}_\infty$  controls. Table 3 presents the values of the two

Table 3

Comparison of transfer function norms  $\|T_{xw}\|_2$  and  $\|T_{xw}\|_\infty$  between two types of control for  $\ell = 1$  and  $\alpha = 1$ <sup>a</sup>

|                      | $Re$ | $\ T_{xw}\ _2$ | $\ T_{xw}\ _\infty$ | $\Delta_2$ | $\Delta_\infty$ |
|----------------------|------|----------------|---------------------|------------|-----------------|
| $\mathcal{H}_2$      | 60   | 8.5            | 20.0                | –          | –               |
|                      | 100  | 40.9           | 224.8               | –          | –               |
|                      | 150  | 5541           | 17119               | –          | –               |
|                      | 200  | 5,454,553      | 13,076,172          | –          | –               |
| $\mathcal{H}_\infty$ | 60   | 10.3           | 11.7                | +21.2%     | –41.5%          |
|                      | 100  | 70.3           | 103.6               | +71.9%     | –53.9%          |
|                      | 150  | 6385           | 8594                | +15.2%     | –49.8%          |
|                      | 200  | 5,465,686      | 6,625,000           | +0.2%      | –49.3%          |

<sup>a</sup>  $\mathcal{H}_2$  control and  $\mathcal{H}_\infty$  control with the smallest value possible for  $\gamma$ .  $\Delta_2$  is the relative difference between the transfer function 2-norms and  $\Delta_\infty$  the relative difference between the transfer function  $\infty$ -norms. In all cases,  $\mathcal{H}_\infty$  control improves (reduces) the worst-case disturbance rejection,  $\|T_{xw}\|_\infty$ , while it deteriorates (increases) the rejection of gaussian disturbances  $\|T_{xw}\|_2$ . Also note that, even though the stabilizability limit of this system is  $Re_c = 235$ , the transfer function norms of the controlled system at  $Re \gtrsim 200$  are so large that practical operation of the system in a noisy environment is not possible in this range.

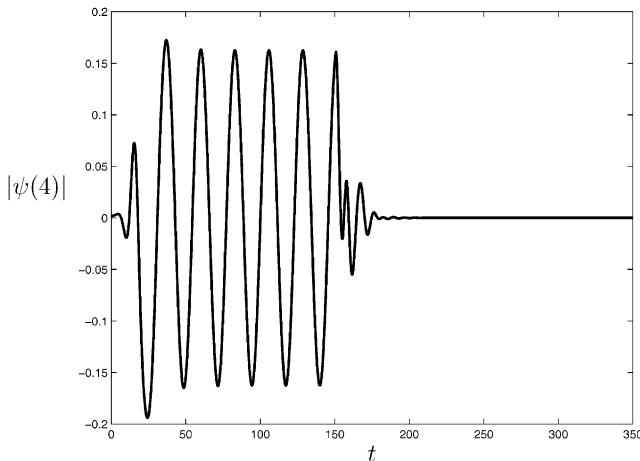


Fig. 4. Linear control of the nonlinear GL equation for  $Re = 100$ : time evolution of the amplitude 4 diameters downstream of the cylinder under white noise conditions. The  $\mathcal{H}_2$  control is switched on at  $t = 150$  and quickly drives the oscillating state to zero.

transfer function norms for various Reynolds numbers with the two control strategies applied: the  $\mathcal{H}_2$  control and the  $\mathcal{H}_\infty$  control with the smallest possible value for  $\gamma$  (termed  $\gamma_0$ ). These computations were achieved with moderate values of both the control penalty ( $\ell = 1$ ) and the measurement noise to state disturbance ratio ( $\alpha = 1$ ). Important conclusions can be drawn from the results displayed on the Table 3. It appears first that both transfer function norms increase monotonically as the Reynolds number is increased, indicating heightened sensitivity of the closed-loop system to disturbances as the number of linear global modes increases. It appears also that applying  $\mathcal{H}_\infty$  control instead of  $\mathcal{H}_2$  control results in an increase in  $\|T_{xw}\|_2$  and a decrease in  $\|T_{xw}\|_\infty$ . As a consequence, a design trade-off should be considered between white disturbance rejection and worst-case disturbance rejection. It is also apparent that, for increasing  $Re$ , it is preferable to apply  $\mathcal{H}_\infty$  control than  $\mathcal{H}_2$  control, as the  $\mathcal{H}_\infty$  approach gives a very large decrease in  $\|T_{xw}\|_\infty$ , denoted  $\Delta_\infty$ , while giving only a very small increase in  $\|T_{xw}\|_2$ , denoted  $\Delta_2$ . We thus conclude that applying a robust control strategy as one approaches the stabilizability limit of the system,  $Re = 235$ , presents a substantial advantage over the corresponding optimal control strategy.

#### 4.2. Linear control of the nonlinear GL equation

The idea of applying the linear control strategy to the nonlinear GL model is appealing for two reasons: first, because having designed and computed a linear control strategy, it is straightforward to test it on the nonlinear equation, and second, because the nonlinear model better addresses the real problem of interest, that is,

stabilizing the nonlinear synchronized behavior. Fig. 4 displays a simulation for  $Re = 100$  with random finite-amplitude initial conditions for the simulation when the linear optimal control is applied at time  $t = 150$ . This simulation was performed with a semi-implicit Adams–Bashforth–Crank–Nicholson time advancement under white noise conditions. It can be seen in Fig. 4 that linear control effectively stabilizes the nonlinear system and drives the state to zero extremely quickly. Further computations will be needed to explore this result at different Reynolds numbers and for various different control strategies, though this preliminary result is encouraging in this regard.

## 5. Conclusion

This paper investigates the use of linear  $\mathcal{H}_\infty$  control theory on a simple model of the cylinder wake to broach some fundamental unanswered questions regarding the control of open shear flows instabilities. It is shown that the application of such modern control rules leads to substantially better performance than the proportional measurement feedback proposed by previous studies by delaying the Reynolds number for onset of linear global instability by a factor of 5 and significantly decreasing the sensitivity of the system to external perturbations. The advantage of using robust over optimal control was shown to be of particular importance near the stabilizability limit of the system, and preliminary results were given where the linear control stabilized the entire nonlinear GL equation.

One of the conclusions from Monkewitz (1989) and Huerre and Monkewitz (1990) concerning control of open flows was that it was very likely that each linear global mode needed to be stabilized by a separate actuator/sensor pair. The present paper has shown that, with the proper control algorithm, this is in fact not the case. The present control strategy stabilizes six linear global modes with a single actuator/sensor pair.

Significant fundamental questions still remain unanswered. What is the best position for the actuator and the sensor to obtain an overall best performance, and what is the new maximum Reynolds number and number of global modes which can be stabilized? How is the “stabilizability limit” of the system characterized in terms of its eigenmodes? What is the limiting factor preventing stabilization at higher  $Re$ ? Under what conditions is the linear control effective on the nonlinear equation in the synchronized, self-sustained, limit-cycling behavior? What is the effect of the noncooperative aspect of the “robust” formulation on this problem? What filtering technique is most appropriate for estimation of the nonlinear equation? These questions are currently under active investigation by the authors, and will be reported in future work.

## Acknowledgements

The authors gratefully acknowledge the encouragements and technical advice of Patrick Huerre (Directeur-State) and Jean-Marc Chomaz (Directeur-Adjoint) at LadHyX. The first author acknowledges the funding of CTE, Ecole des Mines de Paris.

## References

- Berger, E., 1967. Suppression of vortex shedding and turbulence behind oscillating cylinders. *Phys. Fluids* 10, S191–S193.
- Bewley, T.R., 2001. Flow control: new challenges for a new renaissance. *Progress in Aerospace Sciences* 37, 21–58.
- Chomaz, J.M., Huerre, P., Redekopp, L.G., 1988. Bifurcations to local and global modes in spatially developing flows. *Phys. Rev. Lett.* 60, 25–28.
- Doyle, J.C., Glover, K., Khargonekar, P.P., Francis, B.A., 1989. State-space solutions to standard  $\mathcal{H}_2$  and  $\mathcal{H}_\infty$  control problems. *IEEE Trans. Aut. Cont.* 34, 831–847.
- He, J.-W., Glowinski, R., Metcalfe, R., Nordlander, A., Periaux, J., 2000. Active control and drag optimization for flow past a circular cylinder I. Oscillatory Cylinder Rotation. *J. Comp. Phys.* 163, 83–117.
- Huerre, P., Monkewitz, P.A., 1990. Local and global instabilities in spatially developing flows. *Ann. Rev. Fluid. Mech.* 22, 473–537.
- Lauga, E., Bewley, T.R., 2002. The decay of stabilizability with Reynolds number in models of spatially developing flows. *Proc. R. Soc.*, submitted.
- Min, C., Choi, H., 1999. Suboptimal feedback control of vortex shedding at low Reynolds numbers. *J. Fluid Mech.* 401, 123–156.
- Monkewitz, P.A., 1989. Feedback control of global oscillations in fluid systems. *AIAA Paper*, 89–0991.
- Park, D.S., Ladd, D.M., Hendricks, E.W., 1994. Feedback control of von Kármán vortex shedding behind a circular cylinder at low Reynolds numbers. *Phys. Fluids* 6, 2390–2405.
- Roussopoulos, K., 1993. Feedback control of vortex shedding at low Reynolds numbers. *J. Fluid Mech.* 248, 267–296.
- Roussopoulos, K., Monkewitz, P.A., 1996. Nonlinear modelling of vortex shedding control in cylinder wakes. *Physica D* 97, 264–273.
- Tokumaru, P.T., Dimotakis, P.E., 1991. Rotary oscillation control of a cylinder wake. *J. Fluid Mech.* 224, 77–90.
- Williamson, C.H.K., 1996. Vortex dynamics in the cylinder wake. *Ann. Rev. Fluid. Mech.* 28, 477–539.